

Signatures of heavy sterile neutrinos at long baseline experiments

Amol Dighe* and Shamayita Ray†

*Tata Institute of Fundamental Research,
Homi Bhabha Road, Colaba, Mumbai 400005, India*

Abstract

Sterile neutrinos with masses ~ 0.1 eV or higher would play an important role in astrophysics and cosmology. We explore possible signatures of such sterile neutrinos at long baseline experiments. We determine the neutrino conversion probabilities analytically in a 4-neutrino framework, including matter effects, treating the sterile mixing angles $\theta_{14}, \theta_{24}, \theta_{34}$, the deviation of θ_{23} from maximality, as well as θ_{13} and the ratio $\Delta m_{\odot}^2 / \Delta m_{atm}^2$ as small parameters for a perturbative expansion. This gives rise to analytically tractable expressions for flavor conversion probabilities from which effects of these parameters can be clearly understood. We numerically calculate the signals at a neutrino factory with near and far detectors that can identify the lepton charge, and point out observables that can discern the sterile mixing signals. We find that clean identification of sterile mixing would be possible for $\theta_{24}\theta_{34} \gtrsim 0.005$ and $\theta_{14} \gtrsim 0.06$ rad with the current bound of $\theta_{13} < 0.2$ rad; a better θ_{13} bound would allow probing smaller values of sterile mixing. We also generalize the formalism for any number of sterile neutrinos, and demonstrate that only certain combinations of sterile mixing parameters are relevant irrespective of the number of sterile neutrinos. This also leads to a stringent test of the scenario with multiple sterile neutrinos that currently is able to describe all the data from the short baseline experiments, including LSND and MiniBOONE.

PACS numbers: 14.60.Pq, 14.60.St

Keywords: sterile neutrinos, long baseline experiments, neutrino factory

*Electronic address: amol@theory.tifr.res.in

†Electronic address: shamayitar@theory.tifr.res.in

I. INTRODUCTION

In the framework of the Standard model (SM) of particle physics, there are only three neutrinos, one each with the electron, muon and tau flavor. The LEP experiments have determined the number of light neutrinos that couple with the Z boson through electroweak interactions to be 2.984 ± 0.008 [1], thus closing the door on any more generations of “active” neutrinos. However, there still may exist sterile neutrinos that do not have electroweak interactions. Though they cannot be detected in the Z decay, they may mix with the active neutrinos and hence participate in neutrino oscillations. The extent of sterile neutrino participation in solar neutrino data is severely restricted from the neutral current data from SNO [2]. The atmospheric neutrino data show that the major contribution to the muon neutrino disappearance has to be from $\nu_\mu \leftrightarrow \nu_\tau$ oscillations, however a small admixture of sterile neutrinos cannot be ruled out [3, 4]. Short baseline experiments sensitive to sterile neutrinos in the ~ 1 eV range [5–8] have given strong upper bounds on sterile mixing. The CNGS experiment expects to further restrict the sterile mixing parameter space through the $\nu_\mu \rightarrow \nu_{e,\tau}$ channels [9]. The MiniBOONE experiment [10] has virtually ruled out any effect of sterile neutrinos in the LSND parameter space [11] if there were only one sterile neutrino species. However, recently it has been pointed out [12] that with two or more sterile neutrinos, it is possible to be in agreement with all the data.

Even if the LSND results are ignored, so that there is no longer any need for sterile neutrinos for explaining the neutrino oscillation data, sterile neutrinos that obey all the constraints from the terrestrial experiments can still play a crucial role in astrophysics and cosmology [13]. The matter enhanced active-sterile neutrino transformation can have a great effect on r-process nucleosynthesis in the core-collapse supernovae [14], and can also influence the explosion dynamics [15]. Moreover, the anisotropy inside the exploding supernova may be transported outside efficiently by sterile neutrinos, thus helping to explain the large observed velocities of pulsars [16]. Sterile neutrinos of mass \sim keV are also excellent dark matter candidates: ν MSM (SM with three sterile neutrinos) [17] manages to explain masses of active neutrinos, baryon asymmetry of the universe and the abundance of dark matter together. The Chandra blank sky observations also allow keV neutrinos to be viable dark matter candidates [18]. Such heavy dark matter also helps in the production of supermassive black holes [19]. Sterile neutrinos may leave their imprints in the supernova neutrino burst

[20, 21], or in the ultrahigh energy neutrino signals observed at the neutrino telescopes [22].

The main requirements for the astrophysically and cosmologically relevant sterile neutrinos are thus that they be heavy ($m \sim 1\text{--}10$ eV for r-process nucleosynthesis, and $m \sim$ keV for the dark matter candidates) and that they mix weakly with the electron and muon neutrino (in order to satisfy the MiniBOONE constraints). In this article, we consider the case with one such sterile neutrino, which may influence neutrino oscillation experiments. We perform the complete 4ν analysis, taking into account all the three additional mixing angles of the sterile neutrino ν_s with the active ones, and the two additional CP violating phases. We only concentrate on heavy neutrinos, such that if m_4 is the mass of the neutrino eigenstate with a dominant sterile component, $\Delta m_{st}^2 \equiv |m_4^2 - m_i^2| \gtrsim 0.1 \text{ eV}^2$ for all other neutrino mass eigenstates ν_i . The oscillations due to Δm_{st}^2 are rather rapid, and can be taken to be averaged out in the long baseline data. As a result, the data are expected to be insensitive to the exact value of Δm_{st}^2 . However, the additional mixing angles θ_{i4} may leave their signatures in the data.

We treat the effects of the sterile neutrino as a perturbation parametrized by a small auxiliary parameter $\lambda \equiv 0.2$. To this end, we represent the active-sterile mixing angles $\theta_{14}, \theta_{24}, \theta_{34}$, the deviation of θ_{23} from maximality, the reactor angle θ_{13} as well as the ratio $\Delta m_{\odot}^2 / \Delta m_{atm}^2$, formally as some power of λ times $\mathcal{O}(1)$ numbers, so that a systematic expansion in powers of λ may be carried out. Averaging out the fast oscillations due to Δm_{st}^2 allows us to obtain simple analytic approximations for the flavor conversion probabilities of neutrinos. The expressions thus obtained describe the dependence of relevant conversion or survival probabilities on the parameters in a transparent manner.

We analyze, using analytical as well as numerical means, how the parameters involving sterile neutrinos – constrained by the data from solar, atmospheric, and short baseline experiments – affect the results at the long baseline experiments. We illustrate this effect quantitatively in the case of a neutrino factory setup involving a near and a far detector that are capable of lepton charge identification. In particular, we consider the CP asymmetry in μ and τ channels as the observables and calculate how far the limits on the sterile mixing parameters can be brought down. We also consider the electron channel, where signals of sterile neutrino mixing can still be established by the counting of the total number of events above a threshold.

The paper is organized as follows. In Sec. II, we explain our formalism of a systematic

expansion of all quantities in an auxiliary small parameter λ and the use of perturbation theory to obtain the neutrino flavor conversion probabilities. In Sec. III we examine some of the possible signatures of sterile neutrino mixing on the signals at a neutrino factory setup with near and far detectors, where we also estimate bounds that can be obtained at such long baseline experiments. In Sec. IV, we generalize our formalism to any number of sterile species and point out that only certain combinations of the sterile mixing parameters are relevant, independent of the number of sterile species. Sec. V concludes.

II. ANALYTIC COMPUTATION OF NEUTRINO FLAVOR CONVERSION PROBABILITIES

We work in the 4- ν framework, where $(\nu_e, \nu_\mu, \nu_\tau, \nu_s)$ form the basis of neutrino flavor eigenstates and $(\nu_1, \nu_2, \nu_3, \nu_4)$ form the basis of neutrino mass eigenstates. The mass eigenstates are numbered according to the convention $|\Delta m_{42}^2| \gg |\Delta m_{32}^2| \gg \Delta m_{21}^2 > 0$, where $\Delta m_{ij}^2 \equiv m_i^2 - m_j^2$. We have $\Delta m_{\text{st}}^2 \approx |\Delta m_{42}^2|$, $\Delta m_{\text{atm}}^2 \approx |\Delta m_{32}^2|$ and $\Delta m_{\odot}^2 \approx \Delta m_{21}^2$. Note that the sign of Δm_{32}^2 is as yet unknown, a positive (negative) Δm_{32}^2 corresponds to the normal (inverted) mass ordering of neutrinos.

The mass and flavor eigenstates of neutrinos are connected through a unitary matrix \mathcal{U} , such that

$$\nu_\alpha = \mathcal{U}_{\alpha i} \nu_i, \quad (1)$$

where $\alpha \in \{e, \mu, \tau, s\}$ and $i \in \{1, 2, 3, 4\}$. The mixing matrix \mathcal{U} may be parametrized as

$$\mathcal{U} = U_{14}(\theta_{14}, \delta_{14}) U_{34}(\theta_{34}, 0) U_{24}(\theta_{24}, \delta_{24}) U_{23}(\theta_{23}, 0) U_{13}(\theta_{13}, \delta_{13}) U_{12}(\theta_{12}, 0), \quad (2)$$

where $U_{ij}(\theta_{ij}, \delta_{ij})$ is the complex rotation matrix in the i - j plane, whose elements $[U_{ij}]_{pq}$ are defined as

$$[U_{ij}(\theta, \delta)]_{pq} = \begin{cases} \cos \theta & p = q = i \text{ or } p = q = j \\ 1 & p = q \neq i \text{ and } p = q \neq j \\ \sin \theta e^{-i\delta} & p = i \text{ and } q = j \\ -\sin \theta e^{i\delta} & p = j \text{ and } q = i \\ 0 & \text{otherwise.} \end{cases} \quad (3)$$

The limit when the sterile neutrino is completely decoupled – or when it does not exist – is obtained simply by putting the mixing angles θ_{14}, θ_{24} and θ_{34} to zero. In this limit, \mathcal{U}

in (2) reduces to the standard Pontecorvo-Maki-Nakagawa-Sakata (PMNS) neutrino mixing matrix. Since we are interested only in oscillation experiments, we neglect any Majorana phases.

We expect θ_{14}, θ_{24} and θ_{34} , the mixing angles involving the sterile neutrino, to be small. Indeed, though the 4ν analysis of atmospheric neutrinos give a rather weak bound of $\theta_{24}^2 \approx |\mathcal{U}_{\mu 4}|^2 < 0.19$ [4], short baseline disappearance experiments [5] constrain $\theta_{24}^2 < 0.013$, whereas the short baseline appearance experiments [6–8, 10] give a bound of $\theta_{14}\theta_{24} \approx |\mathcal{U}_{e4}\mathcal{U}_{\mu 4}| < 0.02$. The atmospheric neutrino data restrict the deviation of θ_{23} from maximality to be < 0.15 rad [23], and the CHOOZ data [24] combined with solar, atmospheric and KamLAND experiments constrain θ_{13} to be less than 0.2 rad [25]. In order to keep track of the smallness of quantities, we introduce an auxiliary number $\lambda \equiv 0.2$ and define the small parameters to be of the form $a\lambda^n$. This allows us to perform a systematic expansion in powers of λ . For the sterile mixing angles, we define

$$\theta_{14} \equiv \chi_{14}\lambda \quad \theta_{24} \equiv \chi_{24}\lambda \quad \theta_{34} \equiv \chi_{34}\lambda \quad , \quad (4)$$

whereas for the active mixing angles, we define

$$\theta_{13} \equiv \chi_{13}\lambda \quad , \quad \theta_{23} \equiv \frac{\pi}{4} + \tilde{\theta}_{23} \equiv \frac{\pi}{4} + \chi_{23}\lambda \quad . \quad (5)$$

Here, all the χ_{ij} are taken to be $\mathcal{O}(1)$ quantities. We also treat the solar mixing angle, $\theta_{12} \approx 0.6$, as an $\mathcal{O}(1)$ quantity. The limits on the other θ_{ij} s mentioned above translate to $\chi_{24} < 0.6$, $\chi_{14}\chi_{24} < 0.5$, $\chi_{23} < 0.75$ and $\chi_{13} < 1$.

In the long baseline neutrino experiments, the dominating term in flavor conversions oscillates as $\sin^2[\Delta m_{\text{atm}}^2 L/(4E)]$. Owing to the small value of $\Delta m_{\odot}^2 L/(4E)$, the oscillations due to Δm_{\odot}^2 do not have enough time to develop, and the effect of Δm_{\odot}^2 may be viewed as a perturbation to the dominating Δm_{atm}^2 oscillations. We treat the ratio $\Delta m_{\odot}^2/|\Delta m_{\text{atm}}^2| \approx 0.03$ as a small parameter, and define

$$\Delta m_{21}^2/\Delta m_{32}^2 \equiv \zeta\lambda^2 \quad . \quad (6)$$

Note that ζ is positive (negative) for the normal (inverted) neutrino mass ordering.

When neutrinos pass through the earth matter, there are matter effects that give rise to an effective potential $V_e = \sqrt{2}G_F N_e$ for the electron neutrino as compared to the other neutrinos by virtue of the its charged current forward scattering interactions. Here G_F is

the Fermi constant and N_e is the number density of electrons. In addition, all the active neutrinos also get an effective potential $V_n = -G_F N_n / \sqrt{2}$ compared to the sterile neutrino by virtue of their neutral current forward scattering reactions. Here N_n is the number density of neutrons. For antineutrinos, the signs of V_e and V_n are reversed. The effective Hamiltonian in the flavor basis is then

$$H_f \approx \frac{1}{2E} \left[\mathcal{U}_0 \begin{pmatrix} -\Delta m_{21}^2 & 0 & 0 & 0 \\ 0 & 0 & 0 & 0 \\ 0 & 0 & \Delta m_{32}^2 & 0 \\ 0 & 0 & 0 & \Delta m_{42}^2 \end{pmatrix} \mathcal{U}_0^\dagger + \begin{pmatrix} A_e + A_n & 0 & 0 & 0 \\ 0 & A_n & 0 & 0 \\ 0 & 0 & A_n & 0 \\ 0 & 0 & 0 & 0 \end{pmatrix} \right], \quad (7)$$

where $A_{e(n)} \equiv 2EV_{e(n)}$, and \mathcal{U}_0 is the mixing matrix in vacuum, whose form is given in (2). Let H_f be diagonalized by a unitary matrix \mathcal{U}_m , such that

$$H_D = \mathcal{U}_m^\dagger H_f \mathcal{U}_m, \quad (8)$$

where H_D is the diagonal matrix. The elements $[H_D]_{ii}$, being the eigenvalues of H_f , give the relative values of $\tilde{m}_i^2/(2E)$, where \tilde{m}_i are the effective masses of the interaction eigenstates in matter. If we assume that the density encountered by the neutrinos during their passage through the earth is a constant, the flavor conversion probabilities may be written in terms of \tilde{m}_i^2 and the elements of \mathcal{U}_m as

$$P_{\alpha\beta} \equiv P(\nu_\alpha \rightarrow \nu_\beta) = \left| \sum_{i,j} [\mathcal{U}_m]_{\alpha i} [\mathcal{U}_m]_{\beta j}^* \exp \left[i \frac{(\tilde{m}_j^2 - \tilde{m}_i^2)L}{2E} \right] \right|^2. \quad (9)$$

This approximation is valid as long as the neutrino trajectories do not pass through the core, and the neutrino energy is not close to the θ_{13} resonance energy in the earth.

In order to calculate \mathcal{U}_m , it is convenient to work in the basis of neutrino mass eigenstates in vacuum. The effective Hamiltonian in this basis is

$$H_v = \mathcal{U}_0^\dagger H_f \mathcal{U}_0 = \frac{1}{2E} \left[\begin{pmatrix} -\Delta m_{21}^2 & 0 & 0 & 0 \\ 0 & 0 & 0 & 0 \\ 0 & 0 & \Delta m_{32}^2 & 0 \\ 0 & 0 & 0 & \Delta m_{42}^2 \end{pmatrix} + \mathcal{U}_0^\dagger \begin{pmatrix} A_e + A_n & 0 & 0 & 0 \\ 0 & A_n & 0 & 0 \\ 0 & 0 & A_n & 0 \\ 0 & 0 & 0 & 0 \end{pmatrix} \mathcal{U}_0 \right], \quad (10)$$

which can be diagonalized by the unitary matrix \tilde{U} defined through

$$\mathcal{U}_m = \mathcal{U}_0 \tilde{U} \quad (11)$$

such that

$$H_D = \tilde{U}^\dagger \mathcal{U}_0^\dagger H_f \mathcal{U}_0 \tilde{U} = \tilde{U}^\dagger H_v \tilde{U} . \quad (12)$$

Using the formal representation of the elements of \mathcal{U}_0 as well as Δm_{21}^2 in terms of λ as shown in eqs. (4), (5), and (6), the matrix H_v can now be expanded formally in powers of λ as

$$H_v = \frac{\Delta m_{32}^2}{2E} [h_0 + \lambda h_1 + \lambda^2 h_2 + \mathcal{O}(\lambda^3)] . \quad (13)$$

The elements of $h_{0,1,2}$ are functions of all the neutrino mixing angles, mass squared differences and CP violating phases in general; the exact expressions are given in Appendix A. All the elements of the matrices h_1 and h_2 are of $\mathcal{O}(1)$ or smaller, so that the techniques of time independent perturbation theory can be used to calculate the eigenvalues and eigenvectors of H_v that are accurate up to $\mathcal{O}(\lambda^2)$. The complete set of four normalized eigenvectors gives the unitary matrix \tilde{U} that diagonalizes H_v through eq. (12). Using eq. (11), one obtains the unitary matrix \mathcal{U}_m that diagonalizes H_f through eq. (8). The matrix \mathcal{U}_m and the eigenvalues of H_v (or H_f) allow us to calculate the neutrino flavor conversion probabilities from eq. (9).

The flavor conversion probabilities of neutrinos, accurate to $\mathcal{O}(\lambda^2)$, obtained by assuming the neutrinos to travel through a constant matter density, are given in Appendix A. These expressions seem rather complicated. However, we can make certain approximations that will simplify these expressions and bring forth some important physical insights. Since we are interested in heavy sterile neutrinos, we may take $|\Delta m_{32}^2| \ll |\Delta m_{42}^2|$. Also, since $|\Delta m_{32}^2 L/E| \sim \mathcal{O}(1)$, we have $|\Delta m_{42}^2 L/E| \gg 1$ and the oscillating terms of the form $\cos(\Delta m_{42}^2 L/E)$ may be averaged out. In the long baseline experiments, we are interested in the energy range 1–50 GeV. Even at the higher end of the energy spectrum, taking the density of the earth mantle to be ≈ 5 g/cc, we get $A_e \approx 2 \times 10^{-2}$ eV² and $A_n \approx -1 \times 10^{-2}$ eV² for neutrinos, so we also approximate $|A_{e,n}| \ll |\Delta m_{42}^2|$ wherever appropriate. With these approximations, the neutrino flavor conversion (or survival) probabilities for an initial ν_μ may be written as

$$P_{\mu e} \approx 2\theta_{13}^2 \Delta_{32}^2 \frac{\sin^2(\Delta_e - \Delta_{32})}{(\Delta_e - \Delta_{32})^2} + \mathcal{O}(\lambda^3) , \quad (14)$$

$$\begin{aligned} P_{\mu\mu} \approx & \cos^2 \Delta_{32} + 4\tilde{\theta}_{23}^2 \sin^2 \Delta_{32} - \Delta_{21} \sin^2 \theta_{12} \sin 2\Delta_{32} \\ & + \frac{\theta_{13}^2 \Delta_{32}}{(\Delta_e - \Delta_{32})^2} \{ -2\Delta_{32} \cos \Delta_{32} \sin \Delta_e \sin(\Delta_e - \Delta_{32}) + \Delta_e (\Delta_e - \Delta_{32}) \sin 2\Delta_{32} \} \\ & - 2\theta_{24}^2 \cos^2 \Delta_{32} + 2\theta_{24}\theta_{34}\Delta_n \cos \delta_{24} \sin 2\Delta_{32} + \mathcal{O}(\lambda^3) , \end{aligned} \quad (15)$$

$$\begin{aligned}
P_{\mu\tau} \approx & \sin^2 \Delta_{32} - 4\tilde{\theta}_{23}^2 \sin^2 \Delta_{32} + \Delta_{21} \sin^2 \theta_{12} \sin 2\Delta_{32} \\
& + \frac{\theta_{13}^2 \Delta_{32}}{(\Delta_e - \Delta_{32})^2} \{2\Delta_{32} \sin \Delta_{32} \cos \Delta_e \sin(\Delta_e - \Delta_{32}) - \Delta_e(\Delta_e - \Delta_{32}) \sin 2\Delta_{32}\} \\
& - (\theta_{24}^2 + \theta_{34}^2) \sin^2 \Delta_{32} - \theta_{24}\theta_{34} (2\Delta_n \cos \delta_{24} + \sin \delta_{24}) \sin 2\Delta_{32} + \mathcal{O}(\lambda^3), \tag{16}
\end{aligned}$$

where we have defined the dimensionless quantities $\Delta_{ij} \equiv \Delta m_{ij}^2 L/(4E)$ and $\Delta_{e,n} \equiv A_{e,n} L/(4E)$ for convenience. The following observations may be made from the above expressions:

- The leading $\mathcal{O}(1)$ terms are of the form $\sin^2 \Delta_{32}$ or $\cos^2 \Delta_{32}$, corresponding to the dominating atmospheric neutrino oscillations. There is no subleading term of $\mathcal{O}(\lambda)$.
- For $P_{\mu e}$, there is no sterile contribution up to $\mathcal{O}(\lambda^2)$. Indeed, the leading order sterile contribution to $P_{\mu e}$ is proportional to $\theta_{24}^2 \theta_{34}^2$, which is $\mathcal{O}(\lambda^4)$.
- In the expression for $P_{\mu\mu}$ or $P_{\mu\tau}$, the first line contains the leading oscillating term as well as the subleading terms due to the deviation of θ_{23} from maximality and due to the nonzero value of Δm_{21}^2 . The next line gives the contribution from θ_{13}^2 , which matches the one obtained in [26]. The last line contains the contribution from sterile neutrinos. Whereas it is enough to have either θ_{24} or θ_{34} nonzero for the sterile mixing to have an effect on $P_{\mu\tau}$, the sterile contribution to $P_{\mu\mu}$ will be present only for nonzero θ_{24} .
- Only one CP violating phase, δ_{24} , is relevant for the flavor conversion probabilities up to this order. The phases δ_{13} and δ_{14} appear only at $\mathcal{O}(\lambda^3)$ or higher. In particular, the CP violating terms proportional to $(\Delta m_{21}^2/\Delta m_{32}^2)\theta_{13}$, as given in [26], are absent since they are of $\mathcal{O}(\lambda^3)$.
- Note that the leading sterile contribution at the long baseline experiments is found to be at $\mathcal{O}(\lambda^2)$. This may be compared with the CP violation in the active sector, whose leading contribution appears at $\mathcal{O}(\lambda^3)$ and the short baseline appearance experiments, whose positive results would appear only at $\mathcal{O}(\lambda^4)$ or higher. The $\mathcal{O}(\lambda^2)$ sterile contribution to $P_{\mu\tau}$, which is proportional to $\sin \Delta_{32}$, is absent in the short baseline appearance experiments where in general $|\Delta_{42}| \sim \mathcal{O}(1)$ and $|\Delta_{32}| \ll 1$, so that $\sin \Delta_{32} \approx 0$.

- When $\Delta_e \approx \Delta_{32}$, the θ_{13} contribution is enhanced due to the factor $(\Delta_e - \Delta_{32})^{-2}$. The analytical approximation is expected to fail in this region since even the higher order terms in θ_{13} may become significant.
- The analytic expressions are not expected to be valid for large L/E where Δ_{21} would become $\mathcal{O}(\lambda)$ and higher order terms in Δ_{21} would also contribute to the probability in (15) and (16) at $\mathcal{O}(\lambda^2)$.
- The probabilities in (14), (15) and (16) do not involve Δm_{st}^2 , and have no information on whether the mainly sterile neutrino ν_4 is heavier or lighter than the other three. This is due to our approximation of averaging out the fast oscillations due to Δm_{st}^2 . This approximation will be more and more accurate as Δm_{st}^2 increases.

The probabilities for the antiparticles are obtained simply by replacing $\Delta_{e,n} \rightarrow -\Delta_{e,n}$ and $\delta_{ij} \rightarrow -\delta_{ij}$. The sterile contribution to the CP violation is therefore given by

$$P_{\mu\mu} - P_{\bar{\mu}\bar{\mu}} \approx (P_{\mu\mu} - P_{\bar{\mu}\bar{\mu}})_{3\nu} + 4\theta_{24}\theta_{34}\Delta_n \cos \delta_{24} \sin 2\Delta_{32} , \quad (17)$$

$$P_{\mu\tau} - P_{\bar{\mu}\bar{\tau}} \approx (P_{\mu\tau} - P_{\bar{\mu}\bar{\tau}})_{3\nu} - 4\theta_{24}\theta_{34}\Delta_n \cos \delta_{24} \sin 2\Delta_{32} - 2\theta_{24}\theta_{34} \sin \delta_{24} \sin 2\Delta_{32} . \quad (18)$$

The CP violating contribution of sterile neutrinos to $P_{\mu\mu} - P_{\bar{\mu}\bar{\mu}}$ is entirely from the earth matter effects, whereas for $P_{\mu\tau} - P_{\bar{\mu}\bar{\tau}}$, the contribution comes from both the earth matter effects (through the Δ_n term) as well as the vacuum mixing matrix \mathcal{U}_0 (from the $\sin \delta_{24}$ term).

For an initial ν_e , the relevant neutrino flavor conversion probabilities are

$$P_{ee} \approx 1 - 4\theta_{13}^2 \Delta_{32}^2 \frac{\sin^2(\Delta_e - \Delta_{32})}{(\Delta_e - \Delta_{32})^2} - 2\theta_{14}^2 + \mathcal{O}(\lambda^3) , \quad (19)$$

$$P_{e\mu} \approx 2\theta_{13}^2 \Delta_{32}^2 \frac{\sin^2(\Delta_e - \Delta_{32})}{(\Delta_e - \Delta_{32})^2} + \mathcal{O}(\lambda^3) , \quad (20)$$

$$P_{e\tau} \approx 2\theta_{13}^2 \Delta_{32}^2 \frac{\sin^2(\Delta_e - \Delta_{32})}{(\Delta_e - \Delta_{32})^2} + \mathcal{O}(\lambda^3) , \quad (21)$$

where we have used the approximations $|\Delta_{e,n}| \ll |\Delta_{42}|$, and have averaged out terms that oscillate as fast as $\sin \Delta_{42}$. The complete expressions accurate to $\mathcal{O}(\lambda^2)$ may be found in Appendix A. Clearly, sterile neutrinos have no effect at this order on these probabilities except on P_{ee} , and there is no sterile contribution to the CP violation in any of these three channels.

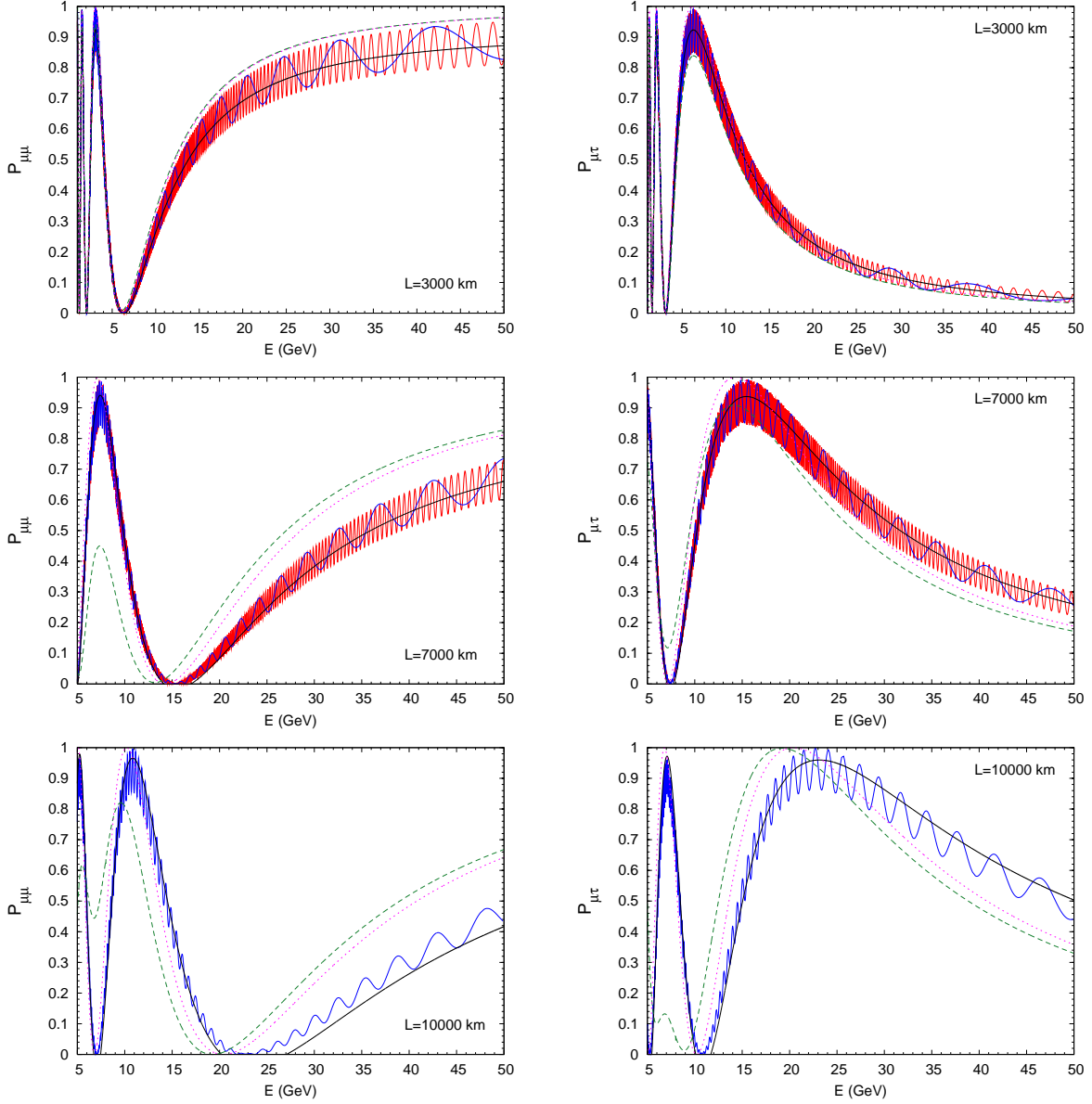


FIG. 1: Probabilities $P_{\mu\mu}$ and $P_{\mu\tau}$ as functions of energy, and the comparisons with the analytic expressions in eqs. (15) and (16). In all the plots, we take $\Delta m_{\odot}^2 = 8 \times 10^{-5} \text{ eV}^2$, $\Delta m_{\text{atm}}^2 = 2.5 \times 10^{-3} \text{ eV}^2$, $\theta_{23} = 45^\circ$, and $\theta_{12} = 33.2^\circ$. The magenta (dotted) curve corresponds to the situation with no sterile contribution and vanishing θ_{13} . The blue (red) curve with rapid (extremely rapid) oscillations corresponds to $\Delta m_{\text{st}}^2 = 0.1$ (1.0) eV^2 , with $\theta_{14} = \theta_{24} = \theta_{34} = 0.2 \text{ rad}$ and $\theta_{13} = 0$. The black curve that passes through the rapidly oscillating curves denotes the analytical approximation, which is independent of the value of Δm_{st}^2 since the high frequency oscillations are averaged out. The green (dashed) curve represents the situation with $\theta_{14} = \theta_{24} = \theta_{34} = 0$, but $\theta_{13} = 0.2 \text{ rad}$.

We demonstrate the validity (and limitations) of our analytic approximations in Fig. 1, where we show $P_{\mu\mu}$ and $P_{\mu\tau}$ as a function of energy for three baselines, 3000 km, 7000 km and 10000 km. In each panel, we show the probabilities with $\theta_{14} = \theta_{24} = \theta_{34} = 0.2$ rad and $\theta_{13} = 0$, for $\Delta m_{\text{st}}^2 = 0.1 \text{ eV}^2$ and $\Delta m_{\text{st}}^2 = 1 \text{ eV}^2$: the complete 4-neutrino numerical simulation with the Preliminary Reference Earth Model (PREM) [27] for the density of the earth, as well as our analytical approximation that uses the average density along the path of the neutrino and averages out the high frequency approximations.¹ In order to estimate whether nonzero θ_{13} can mimic the signatures of sterile mixing, we also show the probability for all the sterile mixing angles vanishing, but $\theta_{13} = 0.2$ rad.

The following observations may be made:

- The analytical approximation agrees well with the average of the exact numerical results for $L = 3000$ km and 7000 km. For $L = 10000$ km, though the analytic approximation predicts the qualitative behavior of the averaged probabilities, the exact numerical values have an error of $\sim 5\%$. This is due to the large L making $\Delta_{21} \sim \mathcal{O}(\lambda)$, so that higher order terms in Δ_{21}^2 contribute to the probabilities (15) and (16).
- The dominant effect of the sterile contribution is to pull down the value of $P_{\mu\mu}$, which mimics the deviation of θ_{23} from its maximal value. Such a mimicking is also possible through a nonzero θ_{13} , however the effect of θ_{i4} may be significantly larger, beyond what is possible with the current limit on θ_{13} . Moreover, at energies much larger than the θ_{13} resonance, the θ_{13} contribution is suppressed by the factor $\Delta_{32}/(\Delta_e - \Delta_{32})$ in earth matter, whereas the sterile contribution does not undergo any suppression since $|\Delta_n| \ll |\Delta_{42}|$ in the whole energy range of interest. One therefore expects that distinguishing the sterile contribution would be easier at high energies.
- Sterile contribution to $P_{\mu\mu}$ as well as $P_{\mu\tau}$ is larger at longer baselines, due to the Δ_n term present in (15) and (16), which increases with increasing L . On the other hand, at low L/E values, the sterile contribution to $P_{\mu\tau}$ is highly suppressed by the factor $\sin \Delta_{32}$ in (16).

¹ For a baseline of 10000 km, we only show $\Delta m_{\text{st}}^2 = 0.1 \text{ eV}^2$, otherwise the oscillation frequency would be too high.

III. SIGNATURES AT LONG BASELINE EXPERIMENTS

The analytical expressions (14)–(16) indicate that at $E \gtrsim 10$ GeV where $|\Delta_e| \gg |\Delta_{32}|$, the contribution of the currently unknown θ_{13} is suppressed by a factor $\sim \Delta_{32}/\Delta_e$. There is no such suppression for the sterile contribution, since $|\Delta_{e,n}| \ll |\Delta_{42}|$ for $E < 50$ GeV. For $E \sim 5$ – 10 GeV, the earth matter effects cause an enhancement of θ_{13} through the factor $\Delta_{32}/(\Delta_e - \Delta_{32})$. This energy range is therefore unsuitable for searching for a sterile contribution to the conversion probabilities. At $E < 5$ GeV also, since the contribution due to the currently unknown θ_{13} is at least of the same order as the maximum allowed sterile contribution, discriminating between θ_{13} and sterile contributions to the probabilities would need data from more than one experiment. A high energy neutrino experiment is therefore preferred.

In order to demonstrate the capability of future long baseline experiments in distinguishing the sterile neutrino contribution to the neutrino flavor conversion probabilities, we choose a typical neutrino factory setup [28], with a 50 GeV muon beam directed to a 0.5 kt “near” detector 1 km away, and a 50 kt “far” detector 7000 km away. The detectors may be magnetized iron calorimeters [29], which can identify the charge of the lepton produced from the charged current interaction of the neutrino or antineutrino. The number of useful muons in the storage ring is taken to be $1.066 \cdot 10^{21}$, which corresponds to approximately two years of running with μ^- and μ^+ each at the neutrino factory, using the NuFact-II parameters in [30]. We implement the propagation of the neutrinos through the earth using the 5-density model of the Earth, where the density of each layer has been taken to be the average of the densities encountered by the neutrinos along their path in that layer with the PREM profile [27]. We take care of the detector characteristics using the General Long Baseline Experiment Simulator (GLOBES) [31]. This includes an energy resolution of $\sigma_E/E = 15\%$, an overall detection efficiency of 75% for all charged leptons, as well as additional energy dependent post-efficiencies that are taken care of bin-by-bin. We assume perfect lepton charge identification, and neglect any error due to wrong sign leptons produced from the oscillations of the antiparticles. These can be taken care of in the complete simulation of the detector once its detailed characteristics are known.

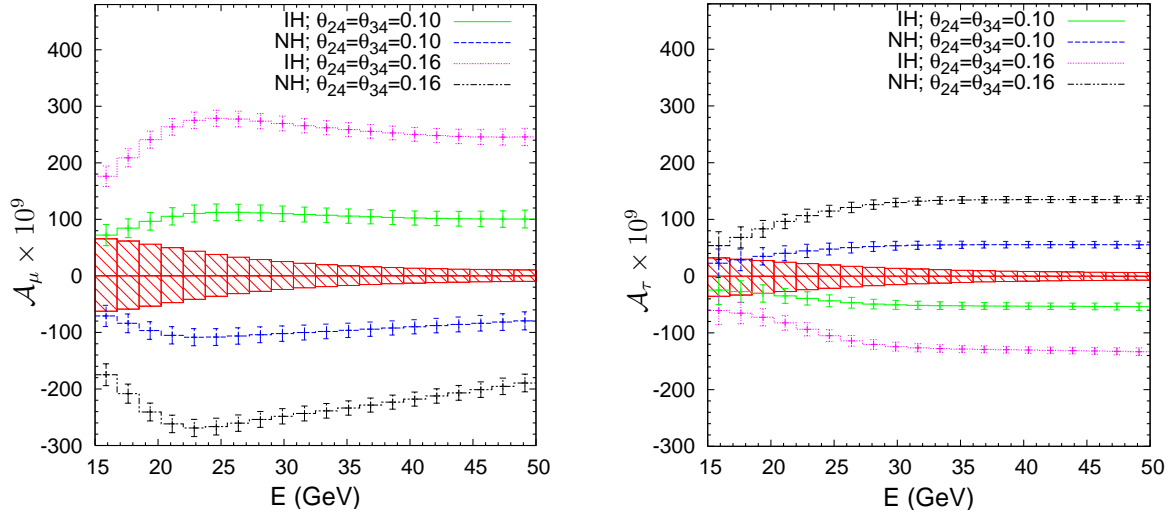


FIG. 2: The asymmetries $\mathcal{A}_\mu(E)$ and $\mathcal{A}_\tau(E)$ as functions of energy at a neutrino factory. The band corresponds to allowed values of the asymmetries without any sterile mixing, with θ_{23} , θ_{13} and δ_{13} allowed to vary over all their allowed ranges, and with both the normal (NH) and inverted (IH) hierarchies. The plots for showing the dependence on sterile components are with $\theta_{23} = \pi/4$, $\delta_{24} = 0$, and $\Delta m_{42}^2 = 0.1 \text{ eV}^2$. The results will not change if Δm_{42}^2 has higher values. No significant dependence on θ_{14} is expected from (15) and (16), hence we use $\theta_{14} = 0$. The errors shown are only statistical.

In Fig. 2, we display the asymmetries

$$\mathcal{A}_\mu(E) \equiv \frac{N_\mu^{\text{far}}(E)}{N_\mu^{\text{near}}(E)} - \frac{\overline{N}_\mu^{\text{far}}(E)}{\overline{N}_\mu^{\text{near}}(E)}, \quad \mathcal{A}_\tau(E) \equiv \frac{N_\tau^{\text{far}}(E)}{N_\mu^{\text{near}}(E)} - \frac{\overline{N}_\tau^{\text{far}}(E)}{\overline{N}_\mu^{\text{near}}(E)}, \quad (22)$$

where N_ℓ (\overline{N}_ℓ) is the number of ℓ^- (ℓ^+) observed at the near or far detector. These asymmetries roughly correspond to $\mathcal{A}_\mu \approx P_{\mu\mu} - P_{\bar{\mu}\bar{\mu}}$ and $\mathcal{A}_\tau \approx P_{\tau\tau} - P_{\bar{\tau}\bar{\tau}}$, where the events observed in the near detector act as a normalizing factor, and help in canceling out the systematic errors due to fluxes, cross sections and efficiencies in each energy bin. Note that we do not expect any τ^\pm at the near detector, hence the number of events of τ^\pm at the far detector needs to be normalized to the number of events of μ^\pm at the near detector.

In the absence of any sterile neutrinos, and in the limit of vanishing θ_{13} , the asymmetries \mathcal{A}_μ and \mathcal{A}_τ vanish, as can be seen from (15) and (16). The θ_{13} contribution is indeed suppressed at high energies, as discussed above. In the figure, we show a band corresponding to the possible signals in the absence of any sterile neutrinos, where we vary over the allowed

values of the angles θ_{23}, θ_{13} , the CP phase δ_{13} and both the normal as well as inverted mass ordering. For $\Delta m_{\text{atm}}^2, \Delta m_{\odot}^2$ and θ_{12} we only take the current best-fit values, since the variation in these parameters is not expected to cause any significant change in our results. We choose to take $\theta_{24} = \theta_{34}$ and $\delta_{24} = 0$ for illustration, since from (17) and (18) we expect the asymmetries to be identical in magnitude and proportional to the product $\theta_{24}\theta_{34}$ with vanishing δ_{24} . Any discrepancy between these two asymmetries would indicate a nonzero δ_{24} , and hence CP violation in the sterile sector. The third sterile mixing angle, θ_{14} , is taken to be vanishing since it is not expected to affect the relevant neutrino conversions.

It may be observed from Fig. 2 that for $E > 15$ GeV, the sterile contribution results in an deficit (excess) of the asymmetry for normal (inverted) hierarchy in the μ channel. In the τ channel, the situation is the reverse. This is as expected from our analytic expressions (17) and (18). The asymmetry integrated over energy may therefore be expected to serve as an efficient discriminator between the scenarios with and without sterile neutrinos. In Fig. 3, we show the integrated asymmetries

$$\begin{aligned}\tilde{\mathcal{A}}_{\mu} &\equiv \frac{N_{\mu}^{\text{far}}(E > 15\text{GeV})}{N_{\mu}^{\text{near}}(E > 15\text{GeV})} - \frac{\overline{N}_{\mu}^{\text{far}}(E > 15\text{GeV})}{\overline{N}_{\mu}^{\text{near}}(E > 15\text{GeV})}, \\ \tilde{\mathcal{A}}_{\tau} &\equiv \frac{N_{\tau}^{\text{far}}(E > 15\text{GeV})}{N_{\mu}^{\text{near}}(E > 15\text{GeV})} - \frac{\overline{N}_{\tau}^{\text{far}}(E > 15\text{GeV})}{\overline{N}_{\mu}^{\text{near}}(E > 15\text{GeV})}.\end{aligned}\quad (23)$$

The figure indicates that for $\theta_{24}\theta_{34} \gtrsim 0.005$, the sterile contribution to neutrino conversions can be discernable from the three neutrino mixing results. The width of the band is determined essentially by the allowed range of θ_{13} . If the value of θ_{13} is bounded further, the reach of neutrino factories for the sterile mixing is enhanced. In addition, the actual value of θ_{13} also affects the discovery potential of sterile mixing by influencing the integrated asymmetries $\tilde{\mathcal{A}}_{\mu}, \tilde{\mathcal{A}}_{\tau}$, as shown in the figure. Note that since the asymmetries depend on the sign of Δm_{32}^2 , sterile mixing also makes it possible to distinguish between normal and inverted hierarchies.

If we have a 50 kt detector that can detect e^-/e^+ and identify their charge², we can use

² Charge identification is needed in order to get rid of the error due to misidentification of the wrong sign leptons produced due to $\nu_{\mu} \rightarrow \nu_e$ or $\bar{\nu}_{\mu} \rightarrow \bar{\nu}_e$ oscillations. A magnetized iron calorimeter with thin iron strips, or a liquid Ar detector [32], may serve the purpose. If charge identification is not possible, as in a water Cherenkov detector for example, the background due to the wrong sign lepton will have to be taken into account.

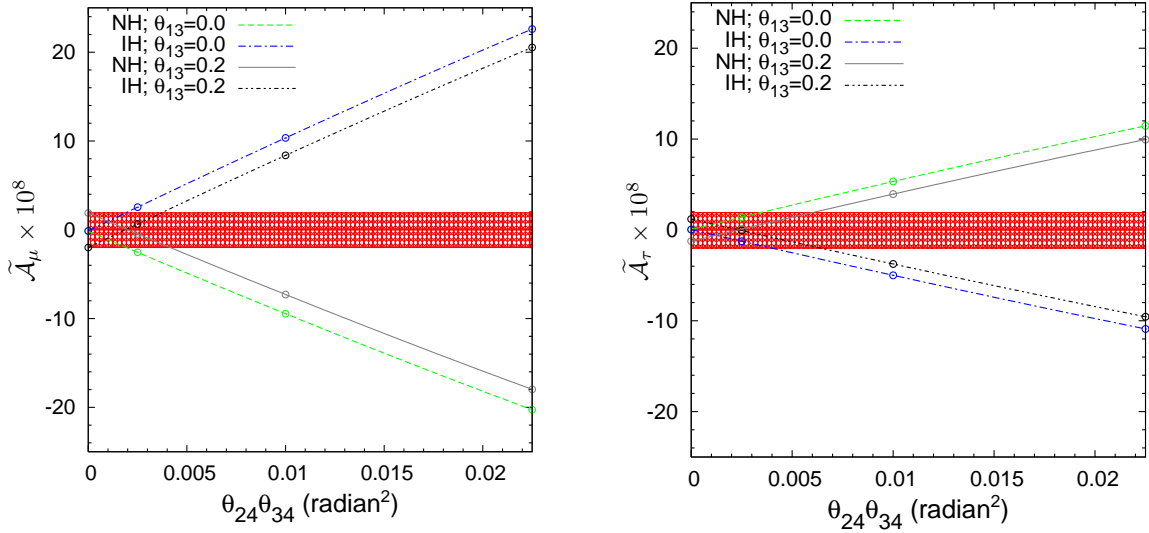


FIG. 3: The integrated asymmetries $\tilde{\mathcal{A}}_\mu$ and $\tilde{\mathcal{A}}_\tau$ as functions of sterile mixing parameters at a neutrino factory. We use $\theta_{24} = \theta_{34}$ and $\delta_{24} = 0$. The rest of the parameters are the same as in Fig. 2. The statistical errors are smaller than the circles shown in the plots.

the observable

$$\mathcal{R}_e(E) \equiv \frac{N_e^{\text{far}}(E)}{N_e^{\text{near}}(E)} \quad (24)$$

and the integrated quantity

$$\tilde{\mathcal{R}}_e \equiv \frac{N_e^{\text{far}}(E > 25\text{GeV})}{N_e^{\text{near}}(E > 25\text{GeV})} \quad (25)$$

for detecting the sterile neutrino contribution. Note that there is no difference between the two hierarchies, or between ν_e and $\bar{\nu}_e$, as far as the expected probabilities are concerned. From Fig. 4, it may be seen that for $\theta_{14} \gtrsim 0.06$, the sterile mixing signals can be clearly discerned. If the bound on θ_{13} becomes stronger, even smaller values of θ_{14} may be identified. On the other hand, an higher actual value of θ_{13} helps in the identification of sterile mixing even at lower θ_{14} values.

The ‘‘platinum’’ channel $P_{\mu e}$ at the neutrino factories is not affected by the sterile mixing, not just to $\mathcal{O}(\lambda^2)$, but even at $\mathcal{O}(\lambda^3)$. Indeed, going to one higher order in the λ -perturbation, we get

$$P_{\mu e} = \frac{\Delta_{32}^2 \sin^2(\Delta_e - \Delta_{32})}{(\Delta_e - \Delta_{32})^2} \left[2\theta_{13}^2 + 4\theta_{13}^2(\tilde{\theta}_{23} - \theta_{13}) \right] + 2\theta_{13}\Delta_{21}\Delta_{32} \sin(2\theta_{12}) \sin \Delta_{32} \frac{\cos(\Delta_e - \Delta_{32} - \delta_{13})}{(\Delta_e - \Delta_{32})} \cdot \frac{\sin \Delta_e}{\Delta_e} + \mathcal{O}(\lambda^4). \quad (26)$$

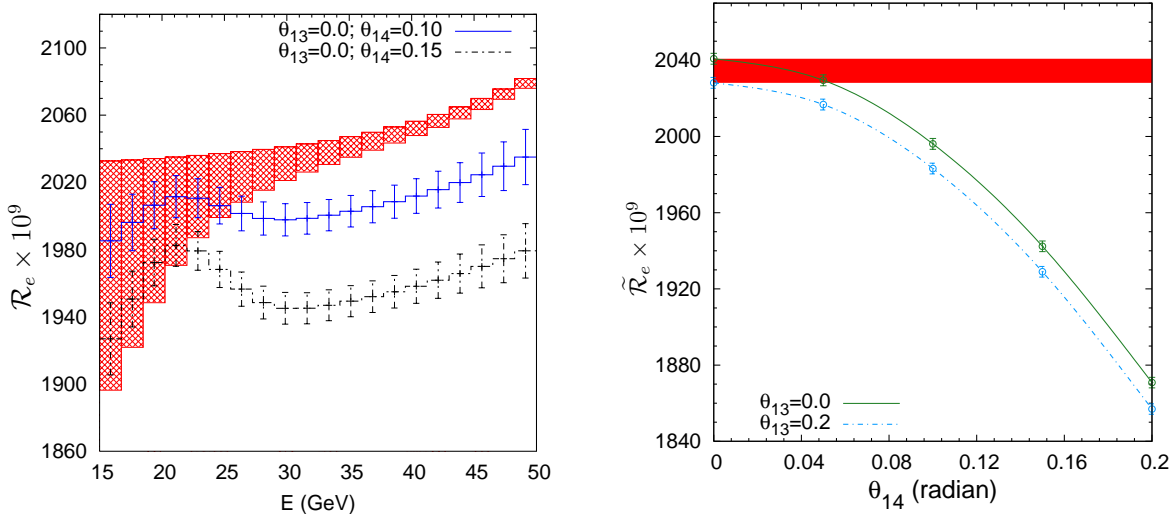


FIG. 4: The observables $\mathcal{R}_e(E)$ and $\tilde{\mathcal{R}}_e$ at a neutrino factory, where e^-/e^+ and their charge may be identified. The active neutrino mixing parameters are the same as that in Fig. 2. The sterile mixing parameters are taken to be $\theta_{24} = \theta_{34} = 0$ and $\Delta m_{42}^2 = 0.1 \text{ eV}^2$. Any increase in Δm_{42}^2 , or nonzero value of θ_{24}/θ_{34} are not expected to have any significant effect on this observable. The result is insensitive to $\text{sgn}(\Delta m_{32}^2)$.

For getting $P_{\bar{\mu}\bar{e}}$, one just needs to replace $\Delta_e \rightarrow -\Delta_e$ and $\delta_{13} \rightarrow -\delta_{13}$. This channel is therefore not expected to be useful in putting constraints on sterile mixing. On the other hand, it is free of any sterile contamination to $\mathcal{O}(\lambda^3)$, and is therefore suitable for determining the parameters in the standard three flavor analysis.

IV. GENERALIZATION TO ANY NUMBER OF STERILE NEUTRINOS

If the LSND results [11] are taken to be valid, a single sterile neutrino is not enough to describe all the data from short baseline experiments. However, two or more sterile neutrinos with $\Delta m_{j1}^2 \sim 1 \text{ eV}$ ($j > 3$) and $|\mathcal{U}_{ej}\mathcal{U}_{\mu j}| \sim \mathcal{O}(0.01-0.1)$ are consistent with all data [12]. Some avenues for probing the mixing parameters and distinguishing between different mass orderings in such a case have already been suggested [21, 33]. It is therefore desirable to extend our formalism to more sterile neutrinos.

The analytical treatment in Sec. II for the case of one sterile neutrino may be generalized easily to any arbitrary number n of sterile neutrinos. The $(3+n) \times (3+n)$ mixing matrix

\mathcal{U} may be written in the block form as

$$\mathcal{U} \equiv \begin{pmatrix} [U^{AA}]_{3 \times 3} & [U^{AS}]_{3 \times n} \\ [U^{SA}]_{n \times 3} & [U^{SS}]_{n \times n} \end{pmatrix} \equiv \mathcal{W} \cdot \mathcal{V} \equiv \begin{pmatrix} [W^{AA}]_{3 \times 3} & [W^{AS}]_{3 \times n} \\ [W^{SA}]_{n \times 3} & [W^{SS}]_{n \times n} \end{pmatrix} \begin{pmatrix} [V^{AA}]_{3 \times 3} & [0]_{3 \times n} \\ [0]_{n \times 3} & [V^{SS}]_{n \times n} \end{pmatrix}, \quad (27)$$

where $V^{AA} \equiv U_{23}(\theta_{23}, 0) U_{13}(\theta_{13}, \delta_{13}) U_{12}(\theta_{12}, 0)$ is the standard mixing matrix for three active neutrino flavors, and V^{SS} is the matrix that mixes the n sterile neutrinos among themselves. Since the assignment of ‘‘flavor’’ eigenstates to the sterile species is arbitrary, we choose the basis such that the flavor and mass eigenstates of the sterile neutrinos coincide in the absence of any active-sterile mixing, i.e. $V^{SS} = I_{n \times n}$. The matrix \mathcal{W} parametrizes the mixing between active and sterile states, and in general may be represented by a product of matrices $U_{ij}(\theta_{ij}, \delta_{ij})$ as defined in eq. (3), with $i \leq 3$ and $j > 3$.

In addition, we assume that all the active-sterile mixing is small, which is borne out by the recent 3+2 neutrino fit to LSND, MiniBOONE as well as the short baseline disappearance data [12]. This allows us to write

$$W^{AS} \equiv \begin{pmatrix} [W^{eS}]_{1 \times n} \\ [W^{\mu S}]_{1 \times n} \\ [W^{\tau S}]_{1 \times n} \end{pmatrix} \equiv \lambda \begin{pmatrix} [X^{eS}]_{1 \times n} \\ [X^{\mu S}]_{1 \times n} \\ [X^{\tau S}]_{1 \times n} \end{pmatrix} \equiv \lambda X^{AS}. \quad (28)$$

If terms of $\mathcal{O}(\lambda^3)$ and smaller are neglected, the unitary matrix \mathcal{W} may be written in its most general form as

$$\mathcal{W} = \begin{pmatrix} \left[I - \lambda^2 \frac{X^{AS}(X^{AS})^\dagger}{2} \right]_{3 \times 3} & [\lambda X^{AS}]_{3 \times n} \\ [-\lambda(X^{AS})^\dagger]_{n \times 3} & \left[I - \lambda^2 \frac{(X^{AS})^\dagger X^{AS}}{2} \right]_{n \times n} \end{pmatrix} + \mathcal{O}(\lambda^3). \quad (29)$$

The net leptonic mixing matrix \mathcal{U} in (27) can then be written as

$$\mathcal{U} = \begin{pmatrix} \left[\left(I - \frac{W^{AS}(W^{AS})^\dagger}{2} \right) V^{AA} \right]_{3 \times 3} & [W^{AS}]_{3 \times n} \\ [-(W^{AS})^\dagger V^{AA}]_{n \times 3} & \left[I - \frac{(W^{AS})^\dagger W^{AS}}{2} \right]_{n \times n} \end{pmatrix} + \mathcal{O}(\lambda^3). \quad (30)$$

For the active mixing angles in V^{AA} , we use the same λ -expansion as in eq. (5), i.e. $\theta_{13} \equiv \chi_{13}\lambda$ and $\theta_{23} \equiv \pi/4 + \tilde{\theta}_{23} \equiv \pi/4 + \chi_{23}\lambda$. We also treat $\Delta m_{21}^2/\Delta m_{32}^2$ to be a small quantity, and denote it formally by $\Delta m_{21}^2/\Delta m_{32}^2 \equiv \zeta\lambda^2$, as in eq. (6). The quantities ζ, χ_{ij} as well as all the elements of X^{AS} are taken to be $\mathcal{O}(1)$ parameters.

Following the same systematic expansion procedure delineated in Sec. II in the case of one sterile neutrino, we obtain the neutrino flavor conversion (or survival) probabilities for an initial ν_μ beam to be

$$P_{\mu e} \approx 2\theta_{13}^2 \Delta_{32}^2 \frac{\sin^2(\Delta_e - \Delta_{32})}{(\Delta_e - \Delta_{32})^2} + \mathcal{O}(\lambda^3), \quad (31)$$

$$\begin{aligned} P_{\mu\mu} \approx & \cos^2 \Delta_{32} + 4\tilde{\theta}_{23}^2 \sin^2 \Delta_{32} - \Delta_{21} \sin^2 \theta_{12} \sin 2\Delta_{32} \\ & + \frac{\theta_{13}^2 \Delta_{32}}{(\Delta_e - \Delta_{32})^2} \{-2\Delta_{32} \cos \Delta_{32} \sin \Delta_e \sin(\Delta_e - \Delta_{32}) + \Delta_e(\Delta_e - \Delta_{32}) \sin 2\Delta_{32}\} \\ & - 2[W^{\mu S}(W^{\mu S})^\dagger] \cos^2 \Delta_{32} + 2\text{Re}[W^{\tau S}(W^{\mu S})^\dagger] \Delta_n \sin 2\Delta_{32} + \mathcal{O}(\lambda^3), \end{aligned} \quad (32)$$

$$\begin{aligned} P_{\mu\tau} \approx & \sin^2 \Delta_{32} - 4\tilde{\theta}_{23}^2 \sin^2 \Delta_{32} + \Delta_{21} \sin^2 \theta_{12} \sin 2\Delta_{32} \\ & + \frac{\theta_{13}^2 \Delta_{32}}{(\Delta_e - \Delta_{32})^2} \{2\Delta_{32} \sin \Delta_{32} \cos \Delta_e \sin(\Delta_e - \Delta_{32}) - \Delta_e(\Delta_e - \Delta_{32}) \sin 2\Delta_{32}\} \\ & - ([W^{\mu S}(W^{\mu S})^\dagger] + [W^{\tau S}(W^{\tau S})^\dagger]) \sin^2 \Delta_{32} \\ & - 2\text{Re}[W^{\tau S}(W^{\mu S})^\dagger] \Delta_n \sin 2\Delta_{32} - \text{Im}[W^{\tau S}(W^{\mu S})^\dagger] \sin 2\Delta_{32} + \mathcal{O}(\lambda^3). \end{aligned} \quad (33)$$

Here we have assumed $|\Delta m_{32}^2|, |A_{e,n}| \ll |\Delta m_{42}^2|$, and have averaged out the oscillating terms of the form $\cos(\Delta m_{42}^2 L/E)$, as before. The sterile contribution to the CP violation in these channels is then

$$P_{\mu\mu} - P_{\bar{\mu}\bar{\mu}} \approx (P_{\mu\mu} - P_{\bar{\mu}\bar{\mu}})_{3\nu} + 4\text{Re}[W^{\tau S}(W^{\mu S})^\dagger] \Delta_n \sin 2\Delta_{32}, \quad (34)$$

$$\begin{aligned} P_{\mu\tau} - P_{\bar{\mu}\bar{\tau}} \approx & (P_{\mu\tau} - P_{\bar{\mu}\bar{\tau}})_{3\nu} - 4\text{Re}[W^{\tau S}(W^{\mu S})^\dagger] \Delta_n \sin 2\Delta_{32} \\ & - 2\text{Im}[W^{\tau S}(W^{\mu S})^\dagger] \sin 2\Delta_{32}. \end{aligned} \quad (35)$$

For an initial ν_e beam, the corresponding flavor conversion probabilities are

$$P_{ee} \approx 1 - 4\theta_{13}^2 \Delta_{32}^2 \frac{\sin^2(\Delta_e - \Delta_{32})}{(\Delta_e - \Delta_{32})^2} - 2[W^{eS}(W^{eS})^\dagger] + \mathcal{O}(\lambda^3), \quad (36)$$

$$P_{e\mu} \approx 2\theta_{13}^2 \Delta_{32}^2 \frac{\sin^2(\Delta_e - \Delta_{32})}{(\Delta_e - \Delta_{32})^2} + \mathcal{O}(\lambda^3), \quad (37)$$

$$P_{e\tau} \approx 2\theta_{13}^2 \Delta_{32}^2 \frac{\sin^2(\Delta_e - \Delta_{32})}{(\Delta_e - \Delta_{32})^2} + \mathcal{O}(\lambda^3). \quad (38)$$

The mixing matrix \mathcal{U} in (30) reduces to the 4×4 mixing matrix \mathcal{U} (2) in the case of one sterile neutrino simply by taking $n = 1$ and using the substitution

$$W^{eS} \rightarrow \theta_{14} e^{-i\delta_{14}}, \quad W^{\mu S} \rightarrow \theta_{24} e^{-i\delta_{24}}, \quad W^{\tau S} \rightarrow \theta_{34}. \quad (39)$$

As a result, the bounds obtained on $\theta_{14}, \theta_{24}, \theta_{34}$ and δ_{24} in the 4-neutrino analysis can be directly translated to bounds on the combinations $[W^{eS}(W^{eS})^\dagger], [W^{\mu S}(W^{\mu S})^\dagger], [W^{\tau S}(W^{\tau S})^\dagger]$ as well as the real and imaginary parts of $[W^{\tau S}(W^{\mu S})^\dagger]$. Note that the expressions (14)–(21) obtained in the special case of only one sterile neutrino can be obtained from the general expressions (31)–(38) simply with the substitutions (39). Specifically, the bounds obtained on $\theta_{24}\theta_{34}$ in Sec. III using the observables $\tilde{\mathcal{A}}_\mu, \tilde{\mathcal{A}}_\tau$ are simply bounds on $\text{Re}[W^{\tau S}(W^{\mu S})^\dagger]$. Similarly, the bound obtained on θ_{14} through \tilde{R}_e is simply the bound on $[W^{eS}(W^{eS})^\dagger]^{1/2}$.

The above argument also implies that, at least in the region of validity of our analytic approximations, the only combinations of active-sterile mixing parameters that may be bounded by data are the four quantities $[W^{eS}(W^{eS})^\dagger], [W^{\mu S}(W^{\mu S})^\dagger], [W^{\tau S}(W^{\tau S})^\dagger]$ and $[W^{\tau S}(W^{\mu S})^\dagger]$, irrespective of the number of sterile species. For example, in the 3+2 scenario, the mixing matrix \mathcal{U} may be written as

$$\begin{aligned} \mathcal{U} = & U_{45}(\theta_{45}, \delta_{45}) \cdot U_{35}(\theta_{35}, \delta_{35}) \cdot U_{25}(\theta_{25}, \delta_{25}) \cdot U_{15}(\theta_{15}, \delta_{15}) \cdot U_{34}(\theta_{34}, \delta_{34}) \cdot \\ & U_{24}(\theta_{24}, \delta_{24}) \cdot U_{14}(\theta_{14}, \delta_{14}) \cdot U_{23}(\theta_{23}, \delta_{23}) \cdot U_{13}(\theta_{13}, \delta_{13}) \cdot U_{12}(\theta_{12}, \delta_{12}), \end{aligned} \quad (40)$$

where $\theta_{45} = 0$, and $\theta_{ij} \sim \mathcal{O}(\lambda)$ for $j > 3$. One may, in addition, choose some of the phases δ_{ij} to be vanishing by proper redefinitions of leptonic phases. With the mixing matrix \mathcal{U} in (40), the substitution

$$\begin{pmatrix} W^{eS} \\ W^{\mu S} \\ W^{\tau S} \end{pmatrix} = \begin{pmatrix} \theta_{14}e^{-i\delta_{14}} & \theta_{15}e^{-i\delta_{15}} \\ \theta_{24}e^{-i\delta_{24}} & \theta_{25}e^{-i\delta_{25}} \\ \theta_{34}e^{-i\delta_{34}} & \theta_{35}e^{-i\delta_{35}} \end{pmatrix} \quad (41)$$

would give the relevant combinations of the sterile mixing parameters:

$$\begin{aligned} [W^{eS}(W^{eS})^\dagger] &= \theta_{14}^2 + \theta_{15}^2, \\ [W^{\mu S}(W^{\mu S})^\dagger] &= \theta_{24}^2 + \theta_{25}^2, \\ [W^{\tau S}(W^{\tau S})^\dagger] &= \theta_{34}^2 + \theta_{35}^2, \\ [W^{\tau S}(W^{\mu S})^\dagger] &= \theta_{24}\theta_{34}e^{i(\delta_{24}-\delta_{34})} + \theta_{25}\theta_{35}e^{i(\delta_{25}-\delta_{35})}. \end{aligned} \quad (42)$$

The expected bounds obtained in Sec. III then would correspond to

$$\theta_{24}\theta_{34} \cos(\delta_{24} - \delta_{34}) + \theta_{25}\theta_{35} \cos(\delta_{25} - \delta_{35}) < 0.005, \quad \sqrt{\theta_{14}^2 + \theta_{15}^2} < 0.06. \quad (43)$$

These bounds will act as a stringent test of the scenario with multiple sterile neutrinos [12].

V. CONCLUSIONS

Heavy sterile neutrinos may play an important role in astrophysics and cosmology, for example in r-process nucleosynthesis or as dark matter. Neutrino oscillation experiments, mainly the short baseline ones, have already put severe constraints on the extent of mixing of these sterile neutrinos with the active ones. If the LSND results are taken to be valid, at least two sterile neutrinos are in fact needed to describe all data.

Our aim in this paper is to check whether the sterile neutrinos so constrained can still give rise to observable signals at future experiments, and whether these signals can be cleanly identified in spite of our current lack of knowledge of all parameters in the mixing of three active neutrinos. This would lead to an estimation of bounds on the sterile mixing parameters that can be obtained with neutrino oscillation experiments.

The number of neutrino mixing parameters increase quadratically with the number of neutrinos, and only certain combinations are expected to be relevant for neutrino flavor conversions. In order to identify these combinations in an analytically tractable manner, we exploit the smallness of certain parameters to carry out a systematic expansion in an arbitrarily defined small parameter, $\lambda \equiv 0.2$. The small quantities $\theta_{14}, \theta_{24}, \theta_{34}, \theta_{13}, \theta_{23} - \pi/4$, and $\Delta m_{\odot}^2/\Delta m_{\text{atm}}^2$ are formally written as powers of λ times $\mathcal{O}(1)$ numbers, and neutrino conversion probabilities correct to $\mathcal{O}(\lambda^2)$ are obtained using techniques of time independent perturbation theory. We also neglect terms proportional to $\Delta m_{\text{atm}}^2/\Delta m_{42}^2$, and average away the fast oscillating terms like $\cos(\Delta m_{42}^2 L/E)$ since $|\Delta m_{42}^2 L/E| \gg 1$ in typical long baseline experiments.

It is observed that the conversion probabilities $P_{\mu e}, P_{e\mu}$ or $P_{e\tau}$ get no sterile contribution to $\mathcal{O}(\lambda^2)$. For $P_{\mu\mu}$ and $P_{\mu\tau}$, sterile mixing gives contributions proportional to θ_{24}^2 and $(\theta_{24}^2 + \theta_{34}^2)$ respectively. In addition, there is a CP violating contribution proportional to $\theta_{24}\theta_{34}$ to both these quantities. The survival probability P_{ee} gets modified simply by a term proportional to θ_{14}^2 . There is no dependence on the mass of the sterile neutrino, since all the terms containing Δm_{42}^2 are averaged out. It is observed that as long as the neutrinos do not pass through the core of the earth, the probabilities obtained through our analytic approximations match the exact numerical ones rather well. Note that the sterile contribution to the conversion probabilities at long baseline experiments appears at $\mathcal{O}(\lambda^2)$, which is at a lower order than the appearance of CP violation in the active sector or the sterile contribution to short

baseline appearance experiments.

Whereas the contribution due to the currently unknown θ_{13} decreases at high energies due to the earth matter effects, the sterile contribution stays almost constant, and therefore the energy range $E = 10\text{--}50$ GeV is suitable for distinguishing the sterile “signal” above the θ_{13} “background”. The CP violating part of the sterile contribution builds up with increasing L , and hence longer baselines are preferable. This naturally leads to the consideration of neutrino factories with $E_\mu = 50$ GeV and baseline of a few thousand km as the desirable setup, with lepton charge identification capability and a near detector for calibration purposes.

For illustration we take the far detector to be near the magic baseline of ≈ 7000 km, and choose three observables, $\tilde{\mathcal{A}}_\mu$ and $\tilde{\mathcal{A}}_\tau$ that correspond to the CP asymmetries in the μ and τ channels respectively, and $\tilde{\mathcal{R}}_e$, which corresponds to the disappearance in the electron channel. The background in these channels is obtained by varying over the unknown values of θ_{13}, θ_{23} and the CP phase δ_{13} . It is observed that the signal rises above this background for $\tilde{\mathcal{A}}_\mu$ and $\tilde{\mathcal{A}}_\tau$ when $\theta_{24}\theta_{34} \gtrsim 0.005$, and for $\tilde{\mathcal{R}}_e$ when $\theta_{14} \gtrsim 0.06$ rad. The range of θ_{i4} probed is limited mainly by the unknown value of θ_{13} . The limit on θ_{13} may be brought down by a factor of two or more at the reactor experiments like Double CHOOZ [34] or Daya Bay [35], and indeed at the neutrino factories themselves [36]. The values of θ_{i4} that can be probed then decrease by approximately the same factor.

Note that we have only chosen to analyze a few specific observables whose dependence on the sterile mixing is analytically transparent. A complete analysis that fits for all the parameters simultaneously may give rise to more stringent constraints. The long baseline experiments thus have the capability of tightening the limits on the sterile mixing angles by almost an order of magnitude over the current ones, or identify sterile neutrinos if their mixing is indeed above such a value. Note that if the sterile mixing is identified through $\tilde{\mathcal{A}}_\mu$ or $\tilde{\mathcal{A}}_\tau$, the neutrino mass hierarchy – normal vs. inverted – is also identified.

In the light of the recent results that show that LSND, MiniBOONE and the earlier null-result short baseline experiments can be consistent if the number of sterile neutrinos is two or more, we have also extended our formalism to include any number of sterile neutrinos. The number of distinct combinations of sterile mixing parameters remains the same, irrespective of the number of sterile neutrinos. We give explicit expressions for such combinations, and the neutrino conversion probabilities in terms of them. The limits obtained on θ_{i4} through the 4ν analysis can easily be translated to the corresponding combinations of these parameters

in the general case. Indeed, the bounds on the sterile mixing parameters obtained from the measurements described in this paper would act as stringent tests of the scenarios with multiple sterile neutrinos.

Acknowledgements

We are grateful to P. Huber for his clear introduction to GLoBES during the JIGSAW07 school and W. Winter for clarifying its further details. We would also like to thank S. Choubey, P. Ghoshal and S. Goswami for useful discussions and insightful comments. This work was partly supported through the Partner Group program between the Max Planck Institute for Physics and Tata Institute of Fundamental Research.

APPENDIX A: FLAVOR CONVERSION PROBABILITIES USING PERTURBATION THEORY TO SECOND ORDER

In order to calculate the neutrino conversion (survival) probabilities in the presence of a sterile neutrino, we define an auxiliary small parameter $\lambda \equiv 0.2$, write all the small quantities as $a\lambda^n$ where a and n are some constants, and then perform a formal expansion of the effective Hamiltonian in powers of λ . This enables us to use the second order perturbation theory to get results accurate to $\mathcal{O}(\lambda^2)$.

We have defined the small quantities in the problem as

$$\theta_{14} = \chi_{14}\lambda, \quad \theta_{24} = \chi_{24}\lambda, \quad \theta_{34} = \chi_{34}\lambda, \quad (\text{A1})$$

$$\theta_{13} = \chi_{13}\lambda, \quad \theta_{23} - \pi/4 = \chi_{23}\lambda, \quad \Delta m_{\odot}^2 / \Delta m_{\text{atm}}^2 = \zeta\lambda^2. \quad (\text{A2})$$

As argued in Sec. II, we need to diagonalize the effective Hamiltonian H_v , given in eq. (10). This Hamiltonian matrix may be expanded in powers of λ as

$$H_v = \frac{\Delta m_{32}^2}{2E} [h_0 + \lambda h_1 + \lambda^2 h_2 + \mathcal{O}(\lambda^3)]. \quad (\text{A3})$$

Here, the leading term is

$$h_0 = \begin{pmatrix} a_n + a_e \cos^2 \theta_{12} & a_e \cos \theta_{12} \sin \theta_{12} & 0 & 0 \\ a_e \cos \theta_{12} \sin \theta_{12} & a_n + a_e \sin^2 \theta_{12} & 0 & 0 \\ 0 & 0 & a_n + 1 & 0 \\ 0 & 0 & 0 & \sigma \end{pmatrix}, \quad (\text{A4})$$

where $a_{e,n} \equiv A_{e,n}/\Delta m_{32}^2$ and $\sigma \equiv \Delta m_{42}^2/\Delta m_{32}^2 \approx \pm \Delta m_{\text{st}}^2/\Delta m_{\text{atm}}^2$. We take the neutrinos to be traversing through a constant matter density, so that $a_{e,n}$ are constants.

The subleading term in (A3) is

$$h_1 = \begin{pmatrix} 0 & 0 & a_e \chi_{13} \cos \theta_{12} e^{-i\delta_{13}} & (a_e + a_n) \chi_{14} e^{-i\delta_{14}} \cos \theta_{12} - \frac{a_n}{\sqrt{2}} \sin \theta_{12} (\chi_{24} e^{-i\delta_{24}} - \chi_{34}) \\ 0 & 0 & a_e \chi_{13} \sin \theta_{12} e^{-i\delta_{13}} & (a_e + a_n) \chi_{14} e^{-i\delta_{14}} \sin \theta_{12} + \frac{a_n}{\sqrt{2}} \cos \theta_{12} (\chi_{24} e^{-i\delta_{24}} - \chi_{34}) \\ \cdot & \cdot & 0 & \frac{a_n}{\sqrt{2}} (\chi_{24} e^{-i\delta_{24}} + \chi_{34}) \\ \cdot & \cdot & \cdot & 0 \end{pmatrix}. \quad (\text{A5})$$

The matrix h_1 is hermitian, so we do not write its lower triangular elements for the sake of brevity. Note that all the elements of h_1 are $\mathcal{O}(1)$.

The expression for the matrix h_2 in (A3) is rather complicated, we just give its ten independent elements separately here for the sake of completeness. The diagonal elements are

$$h_2^{11} = -\Delta_{32}\zeta - [a_e \chi_{13}^2 + (a_e + a_n) \chi_{14}^2] \cos^2 \theta_{12} - \frac{a_n}{2} (\chi_{24}^2 + \chi_{34}^2 - 2\chi_{24}\chi_{34} \cos \delta_{24}) \sin^2 \theta_{12} \\ - \sqrt{2} (a_e + a_n) \chi_{14} [\chi_{34} \cos \delta_{14} - \chi_{24} \cos(-\delta_{14} + \delta_{24})] \sin \theta_{12} \cos \theta_{12},$$

$$h_2^{22} = -[a_e \chi_{13}^2 + (a_e + a_n) \chi_{14}^2] \sin^2 \theta_{12} - \frac{a_n}{2} (\chi_{24}^2 + \chi_{34}^2 - 2\chi_{24}\chi_{34} \cos \delta_{24}) \cos^2 \theta_{12} \\ + \sqrt{2} (a_e + a_n) \chi_{14} [\chi_{34} \cos \delta_{14} - \chi_{24} \cos(-\delta_{14} + \delta_{24})] \sin \theta_{12} \cos \theta_{12},$$

$$h_2^{33} = -\frac{a_n}{2} (\chi_{24}^2 + \chi_{34}^2 + 2\chi_{24}\chi_{34} \cos \delta_{24}) + a_e \chi_{13}^2,$$

$$h_2^{44} = a_n (\chi_{24}^2 + \chi_{34}^2) + (a_e + a_n) \chi_{14}^2, \quad (\text{A6})$$

while the off-diagonal elements are

$$h_2^{12} = \left(-[a_e \chi_{13}^2 + (a_e + a_n) \chi_{14}^2] + \frac{a_n}{2} (\chi_{24}^2 + \chi_{34}^2 - 2\chi_{24}\chi_{34} \cos \delta_{24}) \right) \sin \theta_{12} \cos \theta_{12} \\ + \frac{(a_e + a_n)}{\sqrt{2}} \chi_{14} [\chi_{34} \cos \delta_{14} - \chi_{24} \cos(-\delta_{14} + \delta_{24})] \cos 2\theta_{12} \\ + i \frac{(a_e + a_n)}{2} \chi_{14} [-\chi_{34} \sin \delta_{14} - \chi_{24} \sin(-\delta_{14} + \delta_{24})],$$

$$h_2^{13} = -\frac{(\chi_{24} e^{i\delta_{24}} + \chi_{34})}{2} [\sqrt{2} (a_e + a_n) \chi_{14} e^{-i\delta_{14}} \cos \theta_{12} - a_n (\chi_{24} e^{-i\delta_{24}} - \chi_{34}) \sin \theta_{12}],$$

$$\begin{aligned}
h_2^{23} &= -\frac{(\chi_{24}e^{i\delta_{24}} + \chi_{34})}{2} [\sqrt{2}(a_e + a_n)\chi_{14}e^{-i\delta_{14}} \sin \theta_{12} + a_n(\chi_{24}e^{-i\delta_{24}} - \chi_{34}) \cos \theta_{12}] , \\
h_2^{14} &= \frac{a_n}{\sqrt{2}} (\chi_{24}e^{-i\delta_{24}} + \chi_{34}) (-\chi_{13}e^{-i\delta_{13}} \cos \theta_{12} + \chi_{23} \sin \theta_{12}) , \\
h_2^{24} &= -\frac{a_n}{\sqrt{2}} (\chi_{24}e^{-i\delta_{24}} + \chi_{34}) (\chi_{13}e^{-i\delta_{13}} \sin \theta_{12} + \chi_{23} \cos \theta_{12}) , \\
h_2^{34} &= \frac{a_n}{\sqrt{2}} \chi_{23} (\chi_{24}e^{-i\delta_{24}} - \chi_{34}) + (a_e + a_n) \chi_{13} \chi_{14} e^{i(\delta_{13} - \delta_{14})} . \tag{A7}
\end{aligned}$$

Note that all the elements of h_2 are $\mathcal{O}(1)$ or smaller. The dependence on Δm_{\odot}^2 appears only at this order, and only in the element h_2^{11} .

Using the above formal expansion of the effective Hamiltonian, one can compute the eigenvalues and eigenvectors of H_v correct up to $\mathcal{O}(\lambda^2)$ by using the techniques of time independent perturbation theory. The complete set of four normalized eigenvectors gives the unitary matrix \tilde{U} that diagonalizes H_v through eq. (12). Using eq. (11), we can then compute the unitary matrix \mathcal{U}_m that diagonalizes H_f through eq. (8). The matrix \mathcal{U}_m and the eigenvalues of H_v (or H_f) allow us to calculate the neutrino flavor conversion probabilities from eq. (9). The complete expressions, accurate to $\mathcal{O}(\lambda^2)$, are given below.

$$P_{\mu e} = 2\lambda^2 \chi_{13}^2 \Delta_{32}^2 \frac{\sin^2(\Delta_e - \Delta_{32})}{(\Delta_e - \Delta_{32})^2} + \mathcal{O}(\lambda^3) , \tag{A8}$$

$$\begin{aligned}
P_{\mu\mu} &= \cos^2 \Delta_{32} + 4\lambda^2 \chi_{23}^2 \sin^2 \Delta_{32} - \lambda^2 \zeta \sin^2 \theta_{12} \Delta_{32} \sin 2\Delta_{32} \\
&\quad + \frac{\lambda^2 \chi_{13}^2 \Delta_{32}}{(-\Delta_e + \Delta_{32})^2} \{-2\Delta_{32} \cos \Delta_{32} \sin \Delta_e \sin(\Delta_e - \Delta_{32}) + \Delta_e(\Delta_e - \Delta_{32}) \sin 2\Delta_{32}\} \\
&\quad + \lambda^2 \chi_{24}^2 Q_1 + \lambda^2 \chi_{34}^2 Q_2 + \lambda^2 \chi_{24} \chi_{34} \cos \delta_{24} Q_3 + \mathcal{O}(\lambda^3) , \tag{A9}
\end{aligned}$$

$$\begin{aligned}
P_{\mu\tau} &= \sin^2 \Delta_{32} - 4\lambda^2 \chi_{23}^2 \sin^2 \Delta_{32} + \lambda^2 \zeta \sin^2 \theta_{12} \Delta_{32} \sin 2\Delta_{32} \\
&\quad + \frac{\lambda^2 \chi_{13}^2 \Delta_{32}}{(-\Delta_e + \Delta_{32})^2} \{-2\Delta_{32} \cos \Delta_e \sin \Delta_{32} \sin(\Delta_{32} - \Delta_e) + \Delta_e(-\Delta_e + \Delta_{32}) \sin 2\Delta_{32}\} \\
&\quad + \lambda^2 (\chi_{24}^2 + \chi_{34}^2) Q_4 + \lambda^2 \chi_{24} \chi_{34} (\cos \delta_{24} Q_5 + \sin \delta_{24} Q_6) + \mathcal{O}(\lambda^3) , \tag{A10}
\end{aligned}$$

where we have defined

$$\begin{aligned}
Q_1 &\equiv \frac{1}{4(\Delta_n + \Delta_{32} - \Delta_{42})^2 (-\Delta_n + \Delta_{42})^2} \times \\
&\quad \left\{ -(\Delta_n(\Delta_{32} - 2\Delta_{42}) + 2\Delta_{42}(-\Delta_{32} + \Delta_{42}))^2 \cos 2\Delta_{32} \right. \\
&\quad + (\Delta_n \Delta_{32} - 2(\Delta_n + \Delta_{32})\Delta_{42} + 2\Delta_{42}^2)^2 \cos(2\Delta_n - 2\Delta_{42}) \\
&\quad + 2\Delta_n^2 \Delta_{32} (\Delta_n - \Delta_{42})(\Delta_n + \Delta_{32} - \Delta_{42}) \sin 2\Delta_{32} \\
&\quad \left. - 2(\Delta_n \Delta_{32} - 2(\Delta_n + \Delta_{32})\Delta_{42} + 2\Delta_{42}^2)^2 \sin^2(\Delta_n + \Delta_{32} - \Delta_{42}) \right\} , \tag{A11}
\end{aligned}$$

$$\begin{aligned}
Q_2 \equiv & \frac{\Delta_n^2 \Delta_{32}}{2(\Delta_n + \Delta_{32} - \Delta_{42})^2 (-\Delta_n + \Delta_{42})^2} \times \\
& \left\{ (\Delta_n - \Delta_{42})(\Delta_n + \Delta_{32} - \Delta_{42}) \sin 2\Delta_{32} \right. \\
& \left. - 2\Delta_{32} \cos \Delta_{32} \sin(\Delta_n - \Delta_{42}) \sin(\Delta_n + \Delta_{32} - \Delta_{42}) \right\}, \tag{A12}
\end{aligned}$$

$$\begin{aligned}
Q_3 \equiv & \frac{\Delta_n (\Delta_n (\Delta_{32} - 2\Delta_{42}) + 2\Delta_{42} (-\Delta_{32} + \Delta_{42})) \cos \Delta_{32}}{(\Delta_n + \Delta_{32} - \Delta_{42})^2 (-\Delta_n + \Delta_{42})^2} \times \\
& \left\{ 2(\Delta_n - \Delta_{42})(\Delta_n + \Delta_{32} - \Delta_{42}) \sin \Delta_{32} \right. \\
& \left. + \Delta_{32} [-\cos \Delta_{32} + \cos(2\Delta_n + \Delta_{32} - 2\Delta_{42})] \right\}, \tag{A13}
\end{aligned}$$

$$\begin{aligned}
Q_4 \equiv & \frac{1}{8(\Delta_n + \Delta_{32} - \Delta_{42})^2 (-\Delta_n + \Delta_{42})^2} \left\{ 4\Delta_n (\Delta_{32} - 2\Delta_{42})(\Delta_{32} - \Delta_{42})\Delta_{42} \right. \\
& - 4(\Delta_{32} - \Delta_{42})^2 \Delta_{42}^2 - 2\Delta_n^2 (\Delta_{32}^2 - 2\Delta_{32}\Delta_{42} + 2\Delta_{42}^2) \\
& + 2 \left[-2\Delta_n (\Delta_{32} - 2\Delta_{42})(\Delta_{32} - \Delta_{42})\Delta_{42} + 2(\Delta_{32} - \Delta_{42})^2 \Delta_{42}^2 \right. \\
& \left. + \Delta_n^2 (\Delta_{32}^2 - 2\Delta_{32}\Delta_{42} + 2\Delta_{42}^2) \right] \cos 2\Delta_{32} \\
& + \Delta_n \Delta_{32} \sin \Delta_{32} \left[-8\Delta_n (\Delta_n - \Delta_{42})(\Delta_n + \Delta_{32} - \Delta_{42}) \cos \Delta_{32} \right. \\
& \left. - 4[\Delta_n (\Delta_{32} - 2\Delta_{42}) + 2\Delta_{42} (-\Delta_{32} + \Delta_{42})] \sin(\Delta_{32} - 2\Delta_{42} + 2\Delta_n) \right] \left. \right\}, \tag{A14}
\end{aligned}$$

$$\begin{aligned}
Q_5 \equiv & \frac{\sin \Delta_{32}}{2(\Delta_n + \Delta_{32} - \Delta_{42})^2 (-\Delta_n + \Delta_{42})^2} \times \\
& \left\{ \Delta_n [\Delta_n (\Delta_{32} - 2\Delta_{42}) + \Delta_{42} (-\Delta_{32} + \Delta_{42})] \times \right. \\
& \quad [4(\Delta_n - \Delta_{42})(\Delta_n + \Delta_{32} - \Delta_{42}) \cos \Delta_{32} + 2\Delta_{32} \sin \Delta_{32}] \\
& + 2 \left[-2\Delta_n (\Delta_{32} - 2\Delta_{42})(\Delta_{32} - \Delta_{42})\Delta_{42} + 2(\Delta_{32} - \Delta_{42})^2 \Delta_{42}^2 \right. \\
& \quad \left. + \Delta_n^2 (\Delta_{32}^2 - 2\Delta_{32}\Delta_{42} + 2\Delta_{42}^2) \right] \sin(2\Delta_n + \Delta_{32} - 2\Delta_{42}) \left. \right\}, \tag{A15}
\end{aligned}$$

$$Q_6 \equiv \frac{-4(\Delta_{32} - \Delta_{42})\Delta_{42} \sin(\Delta_n - \Delta_{42}) \sin \Delta_{32} \sin(\Delta_n + \Delta_{32} - \Delta_{42})}{(\Delta_n + \Delta_{32} - \Delta_{42})(-\Delta_n + \Delta_{42})}. \tag{A16}$$

Here we have used the shorthand

$$\Delta_e \equiv \frac{A_e L}{4E_\nu}, \quad \Delta_n \equiv \frac{A_n L}{4E_\nu}, \quad \Delta_{32} \equiv \frac{\Delta m_{32}^2 L}{4E_\nu}, \quad \Delta_{42} \equiv \frac{\Delta m_{42}^2 L}{4E_\nu}. \tag{A17}$$

The probabilities $P_{e\alpha}$ are

$$P_{ee} = 1 - 4\theta_{13}^2\Delta_{32}^2 \frac{\sin^2(\Delta_e - \Delta_{32})}{(\Delta_e - \Delta_{32})^2} - 4\theta_{14}^2\Delta_{42}^2 \frac{\sin^2(\Delta_e + \Delta_n - \Delta_{42})}{(\Delta_e + \Delta_n - \Delta_{42})^2} + \mathcal{O}(\lambda^3), \quad (\text{A18})$$

$$P_{e\mu} = 2\theta_{13}^2\Delta_{32}^2 \frac{\sin^2(\Delta_e - \Delta_{32})}{(\Delta_e - \Delta_{32})^2} + \mathcal{O}(\lambda^3), \quad (\text{A19})$$

$$P_{e\tau} = 2\theta_{13}^2\Delta_{32}^2 \frac{\sin^2(\Delta_e - \Delta_{32})}{(\Delta_e - \Delta_{32})^2} + \mathcal{O}(\lambda^3). \quad (\text{A20})$$

-
- [1] W. M. Yao *et al.* [Particle Data Group], J. Phys. G **33**, 1 (2006).
- [2] Q. R. Ahmad *et al.* [SNO Collaboration], Phys. Rev. Lett. **89**, 011301 (2002) [arXiv:nucl-ex/0204008]; B. C. Chauhan and J. Pulido, JHEP **0412**, 040 (2004) [arXiv:hep-ph/0406227].
- [3] S. Fukuda *et al.* [Super-Kamiokande Collaboration], Phys. Rev. Lett. **85**, 3999 (2000) [arXiv:hep-ex/0009001].
- [4] G. L. Fogli, E. Lisi and A. Marrone, Phys. Rev. D **64**, 093005 (2001) [arXiv:hep-ph/0105139]; T. Nakaya [SUPER-KAMIOKANDE Collaboration], [arXiv:hep-ex/0209036]; D. Choudhury and A. Datta, arXiv:hep-ph/0606100.
- [5] F. Dydak *et al.*, Phys. Lett. B **134**, 281 (1984).
- [6] Y. Declais *et al.* [BUGEY Collaboration], Nucl. Phys. B **434**, 503 (1995).
- [7] B. Armbruster *et al.* [KARMEN Collaboration], Phys. Rev. D **65**, 112001 (2002) [arXiv:hep-ex/0203021].
- [8] P. Astier *et al.* [NOMAD Collaboration], Phys. Lett. B **570**, 19 (2003) [arXiv:hep-ex/0306037].
- [9] A. Donini, M. Maltoni, D. Meloni, P. Migliozzi and F. Terranova, arXiv:0704.0388 [hep-ph].
- [10] A. A. Aguilar-Arevalo *et al.* [The MiniBooNE Collaboration], Phys. Rev. Lett. **98**, 231801 (2007) [arXiv:0704.1500 [hep-ex]].
- [11] A. Aguilar *et al.* [LSND Collaboration], Phys. Rev. D **64**, 112007 (2001) [arXiv:hep-ex/0104049].
- [12] M. Maltoni and T. Schwetz, arXiv:0705.0107 [hep-ph].
- [13] A. Kusenko, AIP Conf. Proc. **917**, 58 (2007) [arXiv:hep-ph/0703116].
- [14] G. C. McLaughlin, J. M. Fetter, A. B. Balantekin and G. M. Fuller, Phys. Rev. C **59**, 2873 (1999) [arXiv:astro-ph/9902106]; J. Fetter, G. C. McLaughlin, A. B. Balantekin and G. M. Fuller, Astropart. Phys. **18**, 433 (2003) [arXiv:hep-ph/0205029].

- [15] J. Hidaka and G. M. Fuller, arXiv:0706.3886 [astro-ph].
- [16] A. Kusenko, Int. J. Mod. Phys. D **13**, 2065 (2004) [arXiv:astro-ph/0409521].
- [17] T. Asaka and M. Shaposhnikov, Phys. Lett. B **620**, 17 (2005) [arXiv:hep-ph/0505013];
T. Asaka, S. Blanchet and M. Shaposhnikov, Phys. Lett. B **631**, 151 (2005) [arXiv:hep-ph/0503065]; N. Sahu and U. A. Yajnik, Phys. Lett. B **635**, 11 (2006) [arXiv:hep-ph/0509285].
- [18] S. Riemer-Sorensen, S. H. Hansen and K. Pedersen, Astrophys. J. **644**, L33 (2006) [arXiv:astro-ph/0603661].
- [19] F. Munyaneza and P. L. Biermann, arXiv:astro-ph/0609388.
- [20] S. Choubey, N. P. Harries and G. G. Ross, Phys. Rev. D **74**, 053010 (2006) [arXiv:hep-ph/0605255].
- [21] S. Choubey, N. P. Harries and G. G. Ross, arXiv:hep-ph/0703092.
- [22] R. L. Awasthi and S. Choubey, arXiv:0706.0399 [hep-ph].
- [23] J. Hosaka *et al.* [Super-Kamiokande Collaboration], Phys. Rev. D **74**, 032002 (2006) [arXiv:hep-ex/0604011].
- [24] M. Apollonio *et al.* [CHOOZ Collaboration], Eur. Phys. J. C **27**, 331 (2003) [arXiv:hep-ex/0301017].
- [25] S. Goswami, A. Bandyopadhyay and S. Choubey, Nucl. Phys. Proc. Suppl. **143**, 121 (2005) [arXiv:hep-ph/0409224].
- [26] E. K. Akhmedov, R. Johansson, M. Lindner, T. Ohlsson and T. Schwetz, JHEP **0404**, 078 (2004) [arXiv:hep-ph/0402175].
- [27] A. M. Dziewonski and D. L. Anderson, Phys. Earth Planet. Interiors **25**, 297 (1981).
- [28] C. H. Albright *et al.* [Neutrino Factory/Muon Collider Collaboration], arXiv:physics/0411123.
- [29] M. S. Athar *et al.* [INO Collaboration], INO-2006-01,
<http://www.imsc.res.in/~ino/OPENReports/INOReport.pdf> .
- [30] P. Huber, M. Lindner and W. Winter, Nucl. Phys. B **645**, 3 (2002) [arXiv:hep-ph/0204352].
- [31] P. Huber, M. Lindner and W. Winter, Comput. Phys. Commun. **167**, 195 (2005) [arXiv:hep-ph/0407333]. P. Huber, J. Kopp, M. Lindner, M. Rolinec and W. Winter, Comput. Phys. Commun. **177**, 432 (2007) [arXiv:hep-ph/0701187].
- [32] A. Ereditato and A. Rubbia, Nucl. Phys. Proc. Suppl. **154**, 163 (2006) [arXiv:hep-ph/0509022];
A. Ereditato and A. Rubbia, Nucl. Phys. Proc. Suppl. **155**, 233 (2006) [arXiv:hep-ph/0510131].
- [33] S. Goswami and W. Rodejohann, arXiv:0706.1462 [hep-ph]; A. Bandyopadhyay and

- S. Choubey, arXiv:0707.2481 [hep-ph].
- [34] F. Ardellier *et al.* [Double Chooz Collaboration], arXiv:hep-ex/0606025.
- [35] X. Guo *et al.* [Daya Bay Collaboration], arXiv:hep-ex/0701029.
- [36] P. Huber, M. Lindner, M. Rolinec and W. Winter, Phys. Rev. D **74**, 073003 (2006) [arXiv:hep-ph/0606119].